RESEARCH ARTICLE

From the Formalism of the Delayed Mackey-Glass Equation and Its Application to Leukemia Growth

Matheus dos Santos Farias[1,*]

[1] Institute for Energy and Nuclear Research (IPEN), University of São Paulo, São Paulo 05508-220, Brazil

Abstract

This study develops a mathematically explicit and computationally reproducible framework based on the delayed Mackey–Glass equation for leukemia-related population dynamics. The classical model is formulated from a population balance law, delayed maturation, and saturating nonlinear feedback, and is then extended by a stage-dependent treatment-control term. Parameters that are not identifiable from the available clinical information are taken from established mathematical and hematopoietic literature, while the treatment-control coefficients are constrained phenomenologically by the modeled burden states. A brief systematic literature search was used to characterize previous Mackey–Glass applications in hematopoiesis and leukemia and to define the methodological gap addressed here. A published case of acute myeloid leukemia-associated myeloid sarcoma treated with radiotherapy and azacitidine provides the clinical treatment schedule and volumetric constraint. The model output is mapped explicitly to a three-dimensional point-cloud representation through a deterministic population-to-point transformation, while the observed reduction from 560 cm^3 to 157 cm^3 after 19.8 Gy provides an independent constraint for a population-to-volume mapping. Sensitivity to the delay and Hill exponent is examined, and the delay-adapted fourth-order Runge–Kutta implementation is compared with an independent adaptive method-of-steps reference. The resulting framework integrates formal derivation, structured literature evidence, treatment modeling, numerical verification, and clinically anchored visualization without presenting the point cloud as a patient-specific radiological reconstruction.

Keywords: Mackey-Glass equation, leukemia growth, delay differential equations, mathematical oncology, radiotherapy, numerical simulation.

1 Introduction

Leukemia remains an important hematological malignancy whose biological dynamics are influenced by proliferation, maturation, feedback regulation, and delayed cellular responses. These mechanisms motivate mathematical models in which the current population depends not only on its present state but also on its previous history. Delay differential

Submitted: 22 July 2026
Revised: 17 August 2026
Accepted: 18 August 2026
Published: 20 September 2026

Vol. 2, **No.** 2, 2026.
10.62762/JNSPM.2026.604346

***Corresponding author:**
✉ Matheus dos Santos Farias
matheusfariasfm@gmail.com

Citation
dos Santos Farias, M. (2026). From the Formalism of the Delayed Mackey-Glass Equation and Its Application to Leukemia Growth. *Journal of Numerical Simulations in Physics and Mathematics*, 2(2), 130–140.

equations are therefore particularly appropriate for representing maturation and regulatory processes that are not instantaneous. Recent epidemiological statistics also underscore the clinical importance of leukemia [1, 2], as summarized in Figure 1.

The Mackey–Glass framework was introduced to represent physiological control systems with delayed feedback and subsequently became a classical model for hematopoiesis. Later studies investigated equilibrium structure, stability, oscillations, bifurcations, parameter identification, and treatment/control in hematopoietic and leukemia-related systems [3–7]. The equation itself is therefore not claimed as a new mathematical object in the present work. Instead, the literature search was used to identify a methodological gap concerning the integration of formal balance-law construction, treatment staging, explicit population-to-point mapping, clinical volume constraints, and numerical verification in one reproducible workflow.

The contribution pursued here is instead the integration of several elements into one reproducible workflow: formal balance-law construction, literature-based parameterization, a treatment-controlled extension, a delay-adapted numerical implementation, and a deterministic mapping from the numerical population to a three-dimensional point-cloud visualization. The approach also distinguishes clinical measurements from model-generated quantities, preventing the synthetic point cloud from being interpreted as a radiological reconstruction.

A published case of acute myeloid leukemia-associated myeloid sarcoma provides a clinically useful reference because it reports lesion dimensions, an initial planning target volume of 560 cm^3, an intermediate volume of 157 cm^3 after 19.8 Gy, a total radiotherapy dose of 30.6 Gy in 17 fractions, and treatment with azacitidine [8]. These data allow the mathematical framework to be connected to a documented therapeutic schedule while preserving the distinction between observed clinical measurements and model outputs.

2 Objectives

2.1 General objective

To develop a mathematically explicit and computationally reproducible Mackey–Glass-based framework for leukemia-related population dynamics and to connect the delayed model to a clinically inspired treatment scenario.

2.2 Specific objectives

- To formulate the delayed population model from a balance law, delayed maturation, and saturating nonlinear feedback.
- To introduce a treatment-controlled extension capable of representing stage-dependent therapeutic reduction.
- To select the baseline Mackey–Glass parameters from established mathematical and hematopoietic literature when the clinical case does not provide sufficient information for unique identification.
- To define a mathematical mapping between the simulated population $P(t)$ and the number and spatial extent of points in the three-dimensional visualization.
- To evaluate sensitivity to the delay τ and Hill exponent n and to verify the numerical implementation against an independent adaptive method-of-steps reference.

3 Materials and Methods

3.1 Clinical basis and data extraction

The clinical reference used in this study is the case report by Majdoul et al. [8], which describes an extramedullary myeloid sarcoma (chloroma) associated with acute myeloid leukemia. The patient received azacitidine together with conformal radiotherapy. The lesion measured $12 \times 7 \times 4$ cm on magnetic resonance imaging, and the initial planning target volume was 560 cm^3. After 19.8 Gy, the planning target volume was reduced to 157 cm^3, permitting adaptive replanning. The total prescribed dose was 30.6 Gy in 17 fractions of 1.8 Gy. These extracted quantities are summarized in Table 1.

The clinical data are deliberately distinguished from model parameters. The reported volumes are observations from the case report. By contrast, β, γ, n, and τ belong to the mathematical model and are selected from established literature or explored numerically. The treatment-control coefficients u_1–u_4 are effective population-level parameters introduced in the present study and constrained so that the modeled burden follows the four stages represented in the visualization. Related delayed hematopoietic and leukemia models have addressed multi-delay stability, CML oscillations, and treatment parameter estimation. The methodological literature also includes established

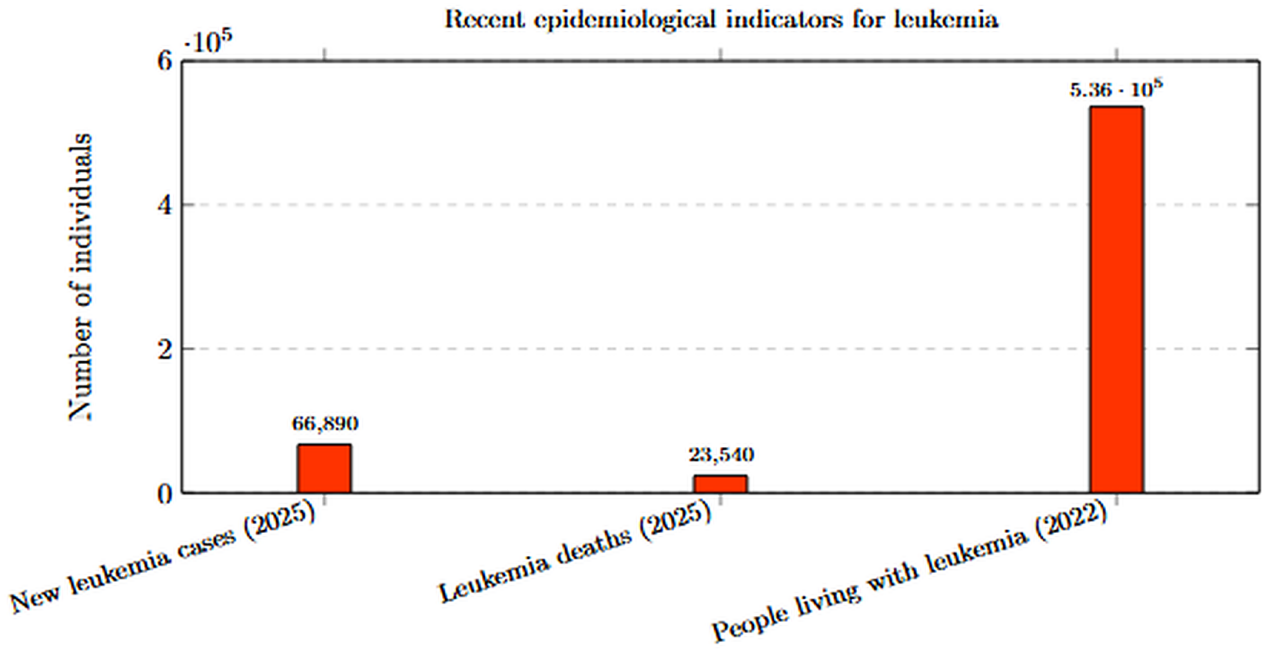

Figure 1. Illustrative epidemiological summary for leukemia based on recent U.S. cancer statistics [1, 2].

Table 1. Clinical quantities extracted from the published myeloid-sarcoma case and their role in the present mathematical formulation.

Clinical quantity	Reported value	Role in the model
Initial planning target volume	560 cm^3	Reference scale for the initial modeled burden
Adaptive-replanning volume	157 cm^3 after 19.8 Gy	Clinical constraint for the population-to-volume mapping
Total radiotherapy dose	30.6 Gy	Defines the treatment horizon
Fractionation	17 fractions × 1.8 Gy	Defines the treatment stages
Adaptive replanning	After 19.8 Gy	Defines the transition to the late-treatment control stage
Systemic treatment	Azacitidine	Included in the effective treatment-control term

numerical DDE methods, Mackey–Glass numerical studies, delayed hematopoietic stability/control analyses, treatment parameter estimation, and leukemia population modeling [9–14].

The 30.6 Gy in 17 fractions schedule is retained because it is the treatment protocol reported in the published case and is not assumed to represent a universal dose standard. International Lymphoma Radiation Oncology Group (ILROG) guidance describes 24 Gy in 12 fractions as a commonly recommended low-dose regimen for myeloid sarcoma, while lower doses may be used in selected clinical situations [15]. Recent reviews report broader dose ranges for radiotherapy of myeloid sarcoma and emphasize that treatment selection depends on the clinical scenario [16]. Thus, the dose stages used here are clinically anchored to the published case and contextualized against radiotherapy literature rather than imposed as a universal therapeutic prescription.

3.1.1 Brief systematic literature search

A brief systematic literature search was conducted on 14 August 2026 to replace the previous manual literature snapshot with a reproducible evidence-identification procedure. PubMed was searched using the Boolean strategy ("Mackey-Glass" OR "Mackey Glass") AND (leukemia OR hematopoiesis OR "chronic myelogenous leukemia") AND (model OR simulation OR stability OR control OR "parameter estimation"). A complementary scholarly-web search was used to identify records not readily indexed under the exact phrase. Eligible records were peer-reviewed studies that (i) used the Mackey–Glass model or a direct mathematical extension, (ii) addressed hematopoiesis or leukemia, and (iii) reported mathematical analysis, numerical simulation, parameter estimation, or treatment/control. Records focused exclusively on respiratory applications, unrelated biological systems, non-mathematical clinical reports, or duplicate publications were excluded. The search was conducted and reported with reference to the PRISMA 2020 reporting guidelines. The retrieved literature consistently showed established use of delayed hematopoietic models for stability, oscillation,

parameter fitting, and leukemia dynamics [17–20]. Because the eligible studies were methodologically heterogeneous, no meta-analysis was attempted, but this subsection is intended as a focused evidence search supporting a research article rather than as a standalone systematic-review manuscript.

3.2 Mathematical formulation

3.2.1 Population balance

Let $P(t)$ denote a normalized measure of the leukemic or hematopoietic population. Over a small time interval Δt, the population variation can be represented as the difference between production and loss:

$$P(t+\Delta t) - P(t) = [\,G(t) - L(t)\,]\,\Delta t. \tag{1}$$

Taking the limit $\Delta t \to 0$ gives the balance law

$$\frac{dP(t)}{dt} = G(t) - L(t). \tag{2}$$

Assuming a first-order loss mechanism, the instantaneous loss is proportional to the current population:

$$L(t) = \gamma\, P(t), \qquad \gamma > 0. \tag{3}$$

3.2.2 Delayed nonlinear feedback

Cell maturation and regulatory signaling introduce a finite delay between the precursor state and the appearance of effective cells. A general representation is obtained through a distributed-memory production term:

$$G(t) = \int_0^\infty K(s)\,\Phi[\,P(t-s)\,]\,ds. \tag{4}$$

Here $K(s)$ is a maturation kernel and Φ is a nonlinear feedback function. When maturation is concentrated around a characteristic delay τ, the kernel can be represented by $K(s) = \delta(s-\tau)$, yielding

$$G(t) = \Phi[\,P(t-\tau)\,]. \tag{5}$$

A saturating feedback can be represented by a Hill-type function. In dimensional form the production function of a population variable P reads

$$\Phi(P) = \frac{\beta\,\theta^n P}{\theta^n + P^n} = \frac{\beta\,P}{1+(P/\theta)^n}, \tag{6}$$

where β is a maximal production scale, θ is a population scale, and n controls the sharpness of the nonlinear feedback. Substitution into the population balance gives the dimensional Mackey–Glass form:

$$\frac{dP}{dt} = \frac{\beta\,P(t-\tau)}{1+\big(P(t-\tau)/\theta\big)^n} - \gamma\,P(t). \tag{7}$$

For the numerical work, P is normalized by θ, with $x(t) = P(t)/\theta$. The equation becomes

$$\frac{dx}{dt} = \frac{\beta\,x(t-\tau)}{1+\big[x(t-\tau)\big]^n} - \gamma\,x(t). \tag{8}$$

3.2.3 Treatment-controlled extension

To represent an effective reduction of the modeled leukemic burden during therapy, the loss term is extended by a non-negative treatment intensity $u(t)$. The resulting model is

$$\frac{dP}{dt} = \frac{\beta\,P(t-\tau)}{1+\big(P(t-\tau)/\theta\big)^n} - \big[\gamma + u(t)\big]\,P(t). \tag{9}$$

The term $u(t)$ is an effective population-level control coefficient. It is not interpreted as a microscopic radiobiological dose-response law or as a direct radiosensitivity parameter. Instead, it summarizes the net reduction associated with the combined therapeutic protocol at each stage. The treatment schedule is represented by four stages:

$$u(t) = \begin{cases} u_1, & 0 \le t < 7, \\ u_2, & 7 \le t < 14, \\ u_3, & 14 \le t < 15.4, \\ u_4, & 15.4 \le t \le 23.8. \end{cases} \tag{10}$$

3.2.4 Equilibrium structure

For the untreated normalized model, a positive equilibrium x^* satisfies

$$0 = \frac{\beta\,x^*}{1+(x^*)^n} - \gamma\,x^*. \tag{11}$$

For $x^* > 0$,

$$x^* = \left[\frac{\beta}{\gamma} - 1\right]^{1/n}, \qquad \beta > \gamma. \tag{12}$$

3.3 Numerical methodology

3.3.1 Delay-adapted fourth-order Runge–Kutta method

The numerical solution uses a classical fourth-order Runge–Kutta formula adapted to the delay term. Because $t-\tau$ is generally not a mesh point, the delayed population is obtained by linear interpolation of previously computed states. A fixed step $h = 0.01$ day is used for the principal simulations. The method is not described as intrinsically superior to all lower-order schemes; its suitability is assessed

through step-size refinement and comparison with an independent adaptive method-of-steps reference [9].

$$P_{k+1} = P_k + \frac{h}{6}\left(K_1 + 2K_2 + 2K_3 + K_4\right). \tag{13}$$

Each K_i evaluates the right-hand side using the interpolated delayed population. As an independent numerical reference, the same delay equation was solved with an adaptive method-of-steps implementation based on `scipy.integrate.solve_ivp`, with the history function and the stage-wise treatment control handled explicitly. This comparison is used to quantify numerical agreement rather than to claim that the two implementations are mathematically identical.

3.3.2 *Parameterization and clinical constraint*

The baseline Mackey–Glass parameters are taken from established literature: $\beta = 0.2$ day^{-1}, $\gamma = 0.1$ day^{-1}, $n = 10$, and $\tau = 20$ days [3–6]. The normalization scale is $\theta = 1$ in the dimensionless numerical formulation. Because the single clinical case does not contain sufficient longitudinal measurements to identify all model parameters independently, the treatment-control coefficients are constrained at the four visualization stages rather than presented as patient-specific microscopic parameters.

$$\frac{V_1}{V_0} = \frac{157}{560} = 0.28036. \tag{14}$$

The population states corresponding to the four visualization stages are $P/P(0) = 1.0000$, 0.65263, 0.35789, and 0.17895. These intermediate normalized population states are model-generated states constrained to the clinically anchored treatment stages; they are not presented as independently observed leukemic cell counts. The clinical evidence directly constrains the treatment timing and dose (9.0, 18.0, 19.8, and 30.6 Gy) and the reported volumetric reduction from 560 cm^3 to 157 cm^3 at 19.8 Gy [8, 15]. The effective stage-control coefficients were obtained numerically so that the delay model reproduces the four modeled burden states at 7, 14, 15.4, and 23.8 days, corresponding to cumulative doses of 9.0, 18.0, 19.8, and 30.6 Gy under the assumption of five fractions per week at 1.8 Gy per fraction. This is described as constrained phenomenological calibration, not full patient-specific parameter estimation. The complete parameter set is listed in Table 2.

Table 2. Parameters used in the treatment-controlled Mackey–Glass simulation.

Parameter	Value	Unit	Origin / role
β	0.2	day^{-1}	Published Mackey–Glass / hematopoiesis literature [3–6]
γ	0.1	day^{-1}	Published Mackey–Glass / hematopoiesis literature [3–6]
n	10	dimensionless	Established Mackey–Glass parameter [3–6]
τ	20	days	Literature-supported baseline; sensitivity tested
θ	1	normalized scale	Dimensionless normalization
u_1	0.0000	day^{-1}	Effective stage-control coefficient, constrained in present study
u_2	0.0897	day^{-1}	Effective stage-control coefficient, constrained in present study
u_3	0.5429	day^{-1}	Effective stage-control coefficient, constrained in present study
u_4	0.4638	day^{-1}	Effective stage-control coefficient, constrained in present study

3.3.3 *Mapping the model solution to the 3D point cloud*

The relationship between the numerical population $P(t)$ and the point-cloud visualization is explicitly defined. Let $N(t)$ be the number of orange points representing the modeled leukemic burden. The baseline number is $N_0 = 950$. Each point therefore represents a fixed visualization unit of the normalized population:

$$N(t) = \mathrm{round}\left[N_0 \frac{P(t)}{P(0)}\right], \qquad N_0 = 950. \tag{15}$$

The spatial extent of the burden is scaled independently through a radius proportional to the cubic root of the normalized population, consistent with a three-dimensional volume interpretation:

$$R(t) = R_0 \left[\frac{P(t)}{P(0)}\right]^{1/3}. \tag{16}$$

To connect the population state to the observed clinical volume without equating a synthetic point count with a radiological volume, a nonlinear population-to-volume mapping is introduced:

$$V(t) = V_0 \left[\frac{P(t)}{P(0)}\right]^{\alpha}. \tag{17}$$

Using $V_0 = 560$ cm^3 and $V(15.4\,\mathrm{d}) = 157$ cm^3 together with the modeled state $P(15.4)/P(0) = 340/950$ gives $\alpha = 1.2374$. The clinical volume reduction is therefore used as an independent constraint on the population-to-volume mapping, whereas the orange point count is a deterministic visualization transformation and is not itself a clinical measurement. The resulting staged quantities are collected in Table 3.

Table 3. Model-derived stages used for the quantitative point-cloud visualization. The 560 cm^3 and 157 cm^3 values are clinical measurements; the other volumes are outputs of the population-to-volume mapping.

Stage	Time	Dose	$P(t)/P(0)$	Model-equivalent volume	Burden points
Baseline	0.0 d	0 Gy	1.0000	560.0 cm^3 (reference)	950
Week 1	7.0 d	9.0 Gy	1.0000	560.0 cm^3 (model mapping)	950
Week 2	14.0 d	18.0 Gy	0.65263	330.2 cm^3 (model mapping)	620
Week 3	15.4 d	19.8 Gy	0.35789	157.0 cm^3 (clinical constraint)	340
Week 4	23.8 d	30.6 Gy	0.17895	66.6 cm^3 (model mapping)	170

3.4 Sensitivity analysis

Sensitivity was evaluated for the two parameters specifically identified as important for delayed dynamics: the delay τ and the Hill exponent n. The baseline $n = 10$ and $\tau = 20$ days were perturbed over $\tau \in \{5, 10, 15, 20\}$ days and $n \in \{8, 9, 10, 11, 12\}$. The analysis is exploratory rather than a statistical uncertainty quantification because the clinical dataset contains only one case and limited longitudinal observations. The resulting final normalized populations are reported in Table 4.

Table 4. Final normalized population $P(23.8\,\mathrm{d})/P(0)$ for the tested combinations of n and τ.

n	$\tau = 5$ **d**	$\tau = 10$ **d**	$\tau = 15$ **d**	$\tau = 20$ **d**
8	0.120	0.233	0.203	0.179
9	0.122	0.237	0.207	0.179
10	0.124	0.240	0.210	0.179
11	0.125	0.243	0.213	0.179
12	0.127	0.244	0.216	0.179

3.5 Numerical verification and convergence

The delay-adapted RK4 solution was compared with the independent adaptive method-of-steps reference over a sequence of decreasing step sizes; the results are summarized in Table 5.

Table 5. Numerical comparison of the delay-adapted RK4 solution with the independent adaptive method-of-steps reference.

RK4 step h (day)	RMSE vs. reference	Maximum error	$P(23.8\,\mathrm{d})/P(0)$
0.02	9.310×10^{-4}	6.342×10^{-3}	0.178964
0.01	9.916×10^{-7}	8.023×10^{-6}	0.178946
0.0025	9.664×10^{-7}	1.016×10^{-5}	0.178946
0.001	9.665×10^{-7}	1.016×10^{-5}	0.178946

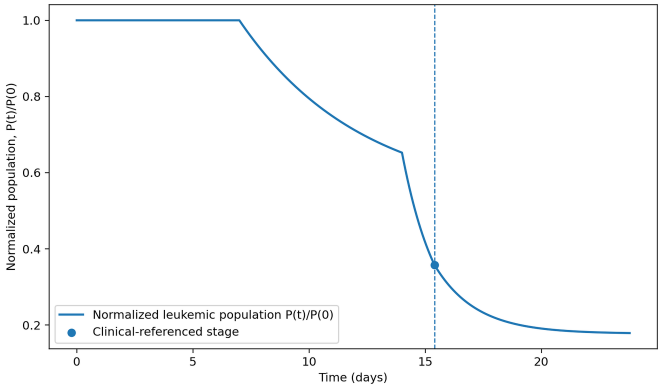

Figure 2. Treatment-controlled Mackey–Glass trajectory. The point at 19.8 Gy corresponds to the clinically reported adaptive-replanning stage; the continuous trajectory is model-generated.

4 Results and Discussion

4.1 Numerical trajectory and clinical constraint

The treatment-controlled Mackey–Glass model produces the staged population trajectory used for the visualization. With the literature-based parameters $\beta = 0.2\,\mathrm{day}^{-1}$, $\gamma = 0.1\,\mathrm{day}^{-1}$, $n = 10$, and $\tau = 20$ days, the first stage remains at the normalized reference state $P/P(0) = 1.0000$. The effective control coefficient then reduces the modeled burden to 0.65263 by 14 days, 0.35789 at the adaptive-replanning point of 19.8 Gy, and 0.17895 by completion of the 30.6 Gy treatment course. The corresponding trajectory is shown in Figure 2.

The agreement between the model state and the clinical volume is deliberately interpreted as a constrained modeling result rather than a direct patient-specific prediction. At 19.8 Gy, the population state $P/P(0) = 0.35789$ is transformed through the calibrated population-to-volume exponent $\alpha = 1.2374$ to reproduce the reported 157 cm^3. This separates the population dynamics from the geometric volume measurement and avoids treating the synthetic point cloud as an imaging reconstruction.

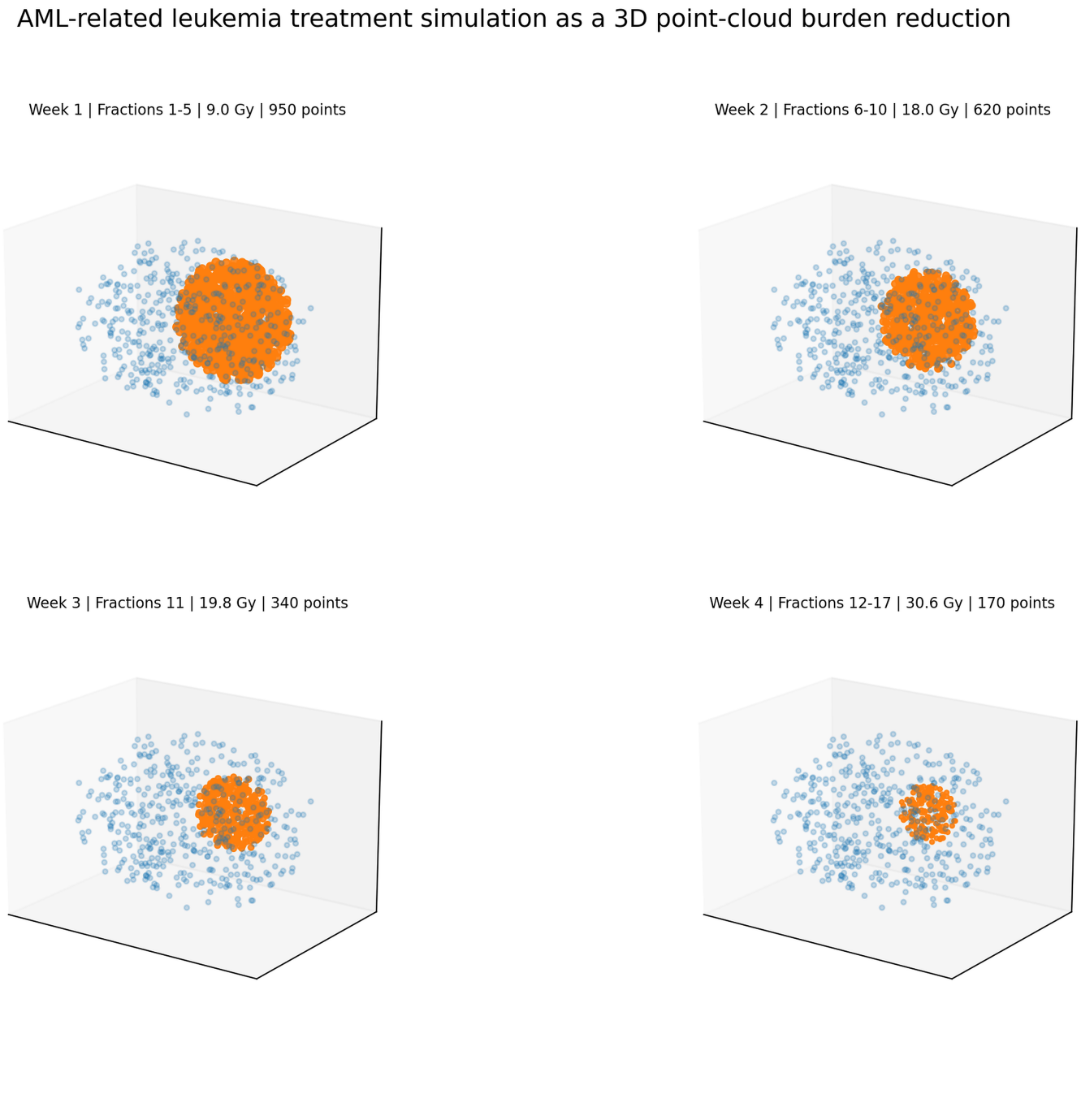

Figure 3. Combined three-dimensional point-cloud simulation of leukemia-related burden reduction during treatment. The four panels correspond to Weeks 1–4 and contain 950, 620, 340, and 170 burden points, respectively.

4.2 Three-dimensional point-cloud representation

The point-cloud simulation is retained as a visualization of the four clinically anchored treatment stages. In the revised formulation, the point counts are no longer arbitrary: they are generated from Eq. (15), so that 950, 620, 340, and 170 points correspond directly to the modeled normalized populations 1.0000, 0.65263, 0.35789, and 0.17895. The treatment stages themselves are anchored by the published radiotherapy schedule, while the point counts are synthetic visualization units. The combined visualization is shown in Figure 3, and the individual weekly states are shown in Figures 4–7.

The point-cloud representation should be interpreted as a population-level visualization. The orange points represent the modeled leukemic burden and the blue points represent a surrounding reference domain. The figures do not reconstruct the patient's anatomy, CT

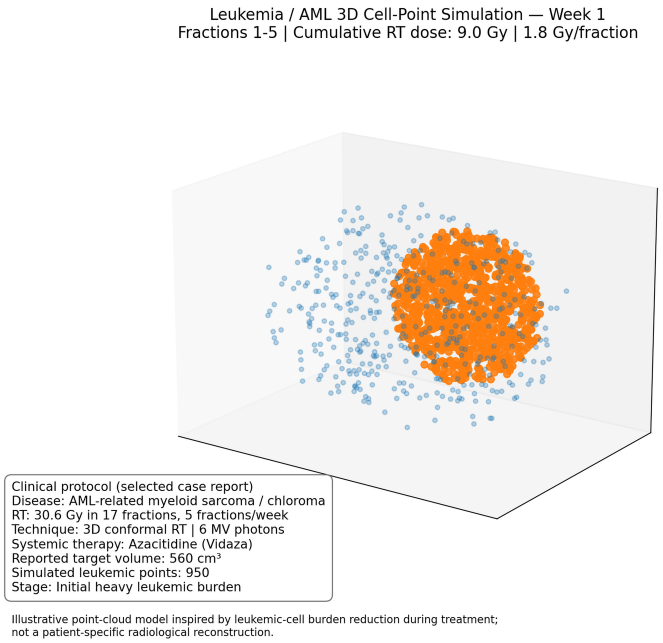

Figure 4. Week 1 point-cloud state: fractions 1–5, cumulative dose 9.0 Gy, and 950 burden points.

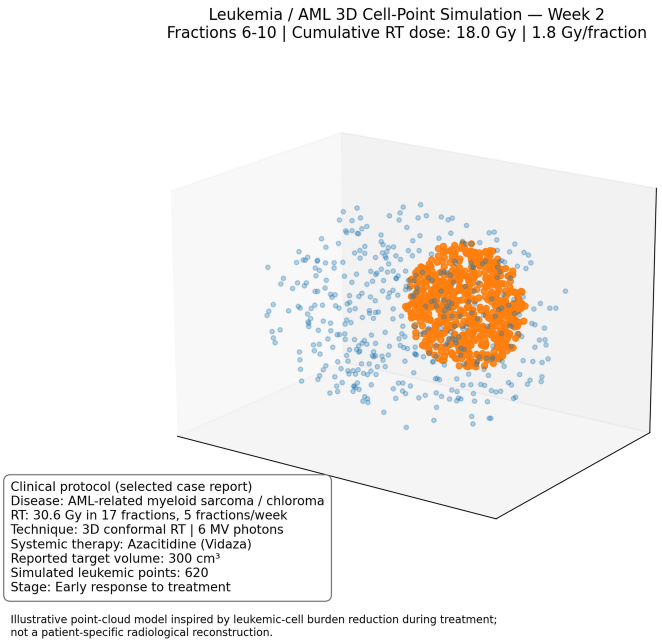

Figure 5. Week 2 point-cloud state: fractions 6–10, cumulative dose 18.0 Gy, and 620 burden points.

volume, MRI segmentation, microscopic cell locations, or radiation dose distribution. Their purpose is to make the temporal reduction of the modeled population visually interpretable.

4.3 Sensitivity to delay and nonlinear feedback

The sensitivity analysis shows that both τ and n affect the final normalized population, but their effects are not equivalent over the tested range. With n fixed, changing the delay from 5 to 20 days modifies the final state substantially (and non-monotonically over the tested grid), whereas changes in n from 8 to 12 produce a more moderate variation for the same delay. This behavior, displayed in Figure 8, is consistent with the role of τ as a direct determinant of the timing of the delayed feedback.

4.4 Numerical verification and convergence

The numerical comparison with the independent adaptive method-of-steps reference provides a direct check of the delay-adapted RK4 implementation. The error decreases markedly as the step size is reduced from 0.02 to 0.01 day and remains at the numerical-reference level for the finer steps used in the verification. The comparison supports the numerical implementation used for the principal simulations without relying on the unsupported claim that RK4 is universally more reliable than lower-order methods for delay equations. The step-size convergence is illustrated in Figure 9.

4.5 Methodological contribution and limitations

The principal contribution of the revised study is not a new Mackey–Glass equation. The equation is established and has been analyzed extensively in hematopoiesis and leukemia-related mathematical modeling [3–6]. The methodological contribution lies in combining formal construction, literature-based parameterization, a stage-dependent treatment-control extension, an explicit population-to-point mapping, a separate population-to-volume constraint, and numerical verification in a single reproducible workflow.

A second contribution is the explicit separation between clinical measurements and model-generated quantities. The clinical report supplies the initial and adaptive-replanning volumes, while the model generates the continuous population trajectory and the synthetic point counts. This distinction prevents the visualization from being presented as if it were a patient-specific radiological reconstruction.

The limitations are important. First, the model uses one clinical case and therefore cannot establish population-level clinical validity. Second, the treatment-control terms are phenomenological and should not be interpreted as microscopic radiosensitivity, radiobiological dose-response, or azacitidine pharmacodynamics. Third, the available case report does not provide enough longitudinal observations for unique estimation of all

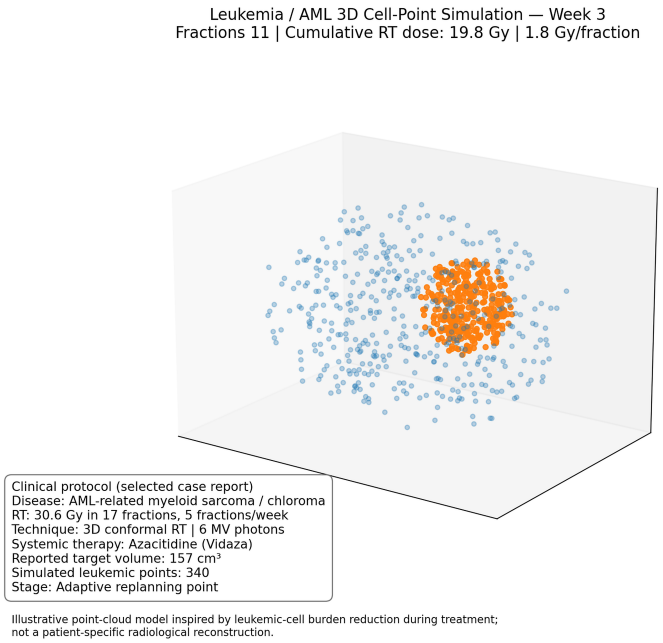

Figure 6. Week 3 point-cloud state: adaptive-replanning point after 19.8 Gy, with 340 burden points.

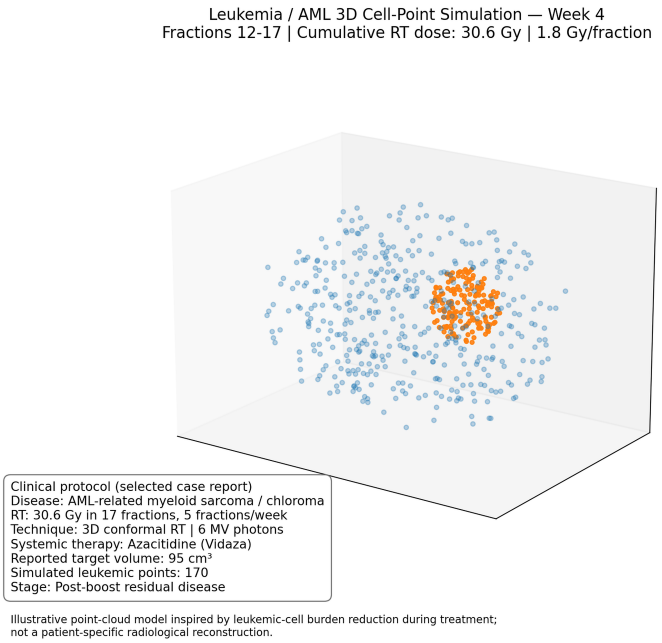

Figure 7. Week 4 point-cloud state: fractions 12–17, cumulative dose 30.6 Gy, and 170 burden points.

Mackey–Glass parameters. Fourth, the point cloud is a qualitative-to-semiquantitative visualization of modeled burden rather than a patient-specific reconstruction. Finally, future studies should test the framework against longitudinal datasets containing repeated volumetric or cellular measurements and compare the effective treatment-control term with mechanistic radiobiological models.

Within these limitations, the revised manuscript provides a mathematically explicit and computationally reproducible proof of concept. The value of the framework is therefore methodological: it demonstrates how a classical delayed population model can be connected to a documented treatment protocol and transformed into an interpretable three-dimensional representation without confusing model output with direct clinical imaging.

5 Conclusion

This study developed a revised Mackey–Glass-based framework for leukemia-related population dynamics that combines formal derivation, literature-based parameterization, treatment control, numerical verification, and three-dimensional visualization. The classical delayed equation was obtained from a population balance law, a distributed maturation mechanism, and a Hill-type nonlinear feedback, while a stage-dependent control term was introduced to represent the effective reduction associated with treatment.

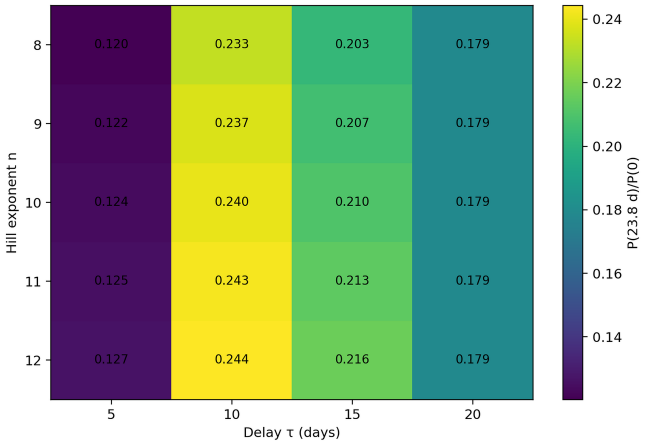

Figure 8. Sensitivity of the final normalized population to the delay τ and Hill exponent n.

The baseline model parameters were taken from established mathematical and hematopoietic literature because the single clinical case does not contain sufficient longitudinal information for unique identification of all Mackey–Glass parameters. The clinical reduction from 560 cm^3 to 157 cm^3 after 19.8 Gy was incorporated as an explicit constraint through a separate population-to-volume mapping, while the number of point-cloud elements was determined directly from the simulated population through a deterministic transformation.

The resulting framework reproduces the four modeled burden states represented in the original visualization and clarifies their mathematical origin. Sensitivity

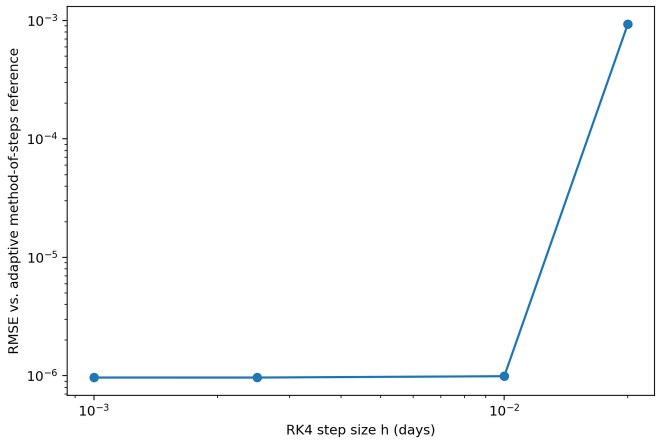

Figure 9. Step-size convergence of the delay-adapted RK4 implementation against an independent adaptive method-of-steps reference.

analysis demonstrates the importance of the delay parameter, and numerical comparison with an independent adaptive method-of-steps reference supports the reliability of the delay-adapted RK4 implementation for the selected simulation settings.

The study should be interpreted as a clinically inspired mathematical proof of concept rather than a validated patient-specific predictor. Its main contribution is the reproducible connection between delayed nonlinear population dynamics, treatment staging, and quantitative visualization, providing a foundation for future work based on larger longitudinal datasets and more mechanistic treatment-response models.

Data Availability Statement

Not applicable.

Funding

This work was supported without any funding.

Conflicts of Interest

The author declares no conflicts of interest.

AI Use Statement

The author declares that no generative AI was used in the preparation of this manuscript.

Ethical Approval and Consent to Participate

This study did not involve recruitment, intervention, or new data collection from human or animal participants. The clinical values used to define the treatment scenario were obtained from a previously published case report and were used only as literature-based clinical constraints for a mathematical simulation. No identifiable patient data were collected or analyzed; therefore, no new ethical approval or informed consent was required for the present simulation study.

References

[1] American Cancer Society. (2025). *Cancer facts & figures 2025*. American Cancer Society. Retrieved from https://www.cancer.org/research/cancer-facts-statistics/all-cancer-facts-figures/2025-cancer-facts-figures.html

[2] National Cancer Institute. (n.d.). *Cancer stat facts: Leukemia*. Surveillance, Epidemiology, and End Results Program. Retrieved from https://seer.cancer.gov/statfacts/html/leuks.html

[3] Mackey, M. C., & Glass, L. (1977). Oscillation and chaos in physiological control systems. *Science, 197*(4300), 287-289. [CrossRef]

[4] Berezansky, L., Braverman, E., & Idels, L. (2013). Mackey-Glass model of hematopoiesis with monotone feedback revisited. *Applied Mathematics and Computation, 219*(9), 4892–4907. [CrossRef]

[5] Berezansky, L., Braverman, E., & Idels, L. (2013). Mackey–Glass model of hematopoiesis with non-monotone feedback: Stability, oscillation and control. *Applied Mathematics and Computation, 219*(11), 6268–6283. [CrossRef]

[6] Adimy, M., Crauste, F., & Ruan, S. (2005). A mathematical study of the hematopoiesis process with applications to chronic myelogenous leukemia. *SIAM journal on applied mathematics, 65*(4), 1328-1352. [CrossRef]

[7] Pujo-Menjouet, L. (2016). Blood cell dynamics: half of a century of modelling. *Mathematical Modelling of Natural Phenomena, 11*(1), 92-115. [CrossRef]

[8] Majdoul, S., Colson-Durand, L., To, N. H., & Belkacemi, Y. (2017). Adaptive radiotherapy for an uncommon chloroma. *Case Reports in Oncology, 9*(3), 593-598. [CrossRef]

[9] Shampine, L. F., & Thompson, S. (2001). Solving ddes in MATLAB. *Applied Numerical Mathematics, 37*(4), 441-458. [CrossRef]

[10] Crauste, F. (2009). Delay model of hematopoietic stem cell dynamics: asymptotic stability and stability switch. *Mathematical Modelling of Natural Phenomena, 4*(2), 28-47. [CrossRef]

[11] Halanay, A., Cândea, D., & Rădulescu, I. R. (2014). Existence and Stability of Limit Cycles in a Two-delays Model of Hematopoiesis Including Asymmetric Division. *Mathematical Modelling of Natural Phenomena, 9*(1), 58-78. [CrossRef]

[12] Badralexi, I., & Halanay, A. (2017, January). Stability and oscillations in a CML model. In *AIP Conference Proceedings* (Vol. 1798, No. 1, p. 020011). AIP Publishing LLC. [CrossRef]

[13] Cândea, D., Halanay, A., Rădulescu, R., & Tălmaci, R. (2017, January). Parameter estimation and sensitivity analysis for a mathematical model with time delays of leukemia. In *AIP Conference Proceedings* (Vol. 1798, No. 1, p. 020034). AIP Publishing LLC. [CrossRef]

[14] Parajdi, L. G., Precup, R., Bonci, E. A., & Tomuleasa, C. (2020). A mathematical model of the transition from normal hematopoiesis to the chronic and accelerated-acute stages in myeloid leukemia. *Mathematics, 8*(3), 376. [CrossRef]

[15] Bakst, R. L., Dabaja, B. S., Specht, L. K., & Yahalom, J. (2018). Use of radiation in extramedullary leukemia/chloroma: guidelines from the International Lymphoma Radiation Oncology Group. *International Journal of Radiation Oncology* Biology* Physics, 102*(2), 314-319. [CrossRef]

[16] Loscocco, G. G., & Vannucchi, A. M. (2023). Myeloid sarcoma: more and less than a distinct entity. *Annals of Hematology, 102*(8), 1973-1984. [CrossRef]

[17] Adimy, M., Crauste, F., & Ruan, S. (2006). Periodic oscillations in leukopoiesis models with two delays. *Journal of Theoretical Biology, 242*(2), 288-299. [CrossRef]

[18] Colijn, C., & Mackey, M. C. (2005). A mathematical model of hematopoiesis—I. Periodic chronic myelogenous leukemia. *Journal of Theoretical Biology, 237*(2), 117-132. [CrossRef]

[19] Safarishahrbijari, A., & Gaffari, A. (2013). Parameter identification of hematopoiesis mathematical model–periodic chronic myelogenous leukemia. *Contemporary Oncology/Współczesna Onkologia, 17*(1), 73-77. [CrossRef]

[20] Foley, C., & Mackey, M. C. (2009). Dynamic hematological disease: a review. *Journal of mathematical biology, 58*(1), 285-322. [CrossRef]

Matheus dos Santos Farias Holds a Bachelor's degree and a teaching qualification in Physics from the Institute of Physics at the University of S~ao Paulo (IF-USP). Conducted research in Applied Physics—specifically within groups focusing on differential equations applied to health, hadron therapy, and cardio-vascular biomechanics—and is a member of the American Physical Society (APS). A specialist in Medical Physics (certified by Albert Einstein Israelite Hospital - HIAE), he has conducted research in proton therapy, delay differential equations, and dynamical systems (chaos theory). His clinical experience covers diagnostic radiology—including quality control, image quality op-timization, and performance assessment for X-ray, CT, mammography, fluoroscopy, and MRI systems—as well as nuclear medicine (involving radiopharmaceuticals, internal dosimetry, and equipment quality control) and radiotherapy (radiotherapy planning, linear accelerator cali-bration, brachytherapy, and dose distribution verification). He also has experience in radiation protection applied to medical physics and is a member of the American Association of Physicists in Medicine (AAPM). Currently pursuing a Master's degree in Nuclear Physics at the Institute for Energy and Nuclear Research (IPEN-USP), he conducts research with an emphasis on de-lay differential equations and dynamical systems (chaos theory). He worked on developing an equation to predict the size of gold nanoparticles (AuNPs) for nanobrachytherapy applications in biomedicine, in international scientific collaboration with University College London (UK). He is a member of the American Nuclear Society (ANS) and the SIAM Activity Group on Dynamical Systems. Laboratory experience in the synthesis of gold (AuNPs), silver (AgNPs), and copper (CuNPs) nanoparticles, as well as their physicochemical characterization using UV-Vis spectroscopy, Dynamic Light Scattering (DLS), Transmission Electron Microscopy (TEM), Scanning Electron Microscopy (SEM), X-Ray Diffraction (XRD), Zeta Potential, and Fourier-Transform Infrared Spectroscopy (FT-IR); expertise in mathematical modeling (analytical and numerical simulation), data analysis, and programming using LaTeX, Python, R, C, C++, MATLAB, Wolfram Mathematica, and Monte Carlo methods (PENELOPE, TOPAS, MCNP); and application of Machine Learning and AI techniques in nuclear, biomedical, and medical fields. (Email: matheusfariasfm@gmail.com)